Supporting Information

Efficient Two-step Synthesis of Water Soluble BODIPY-TREN Chemosensors for Copper(II) Ions

Bram Verbelen,[a] Marlon Valckenborgh,[a] Mario Inclán,‡[b] Aida Nebot[b,] Wim Dehaen*[a] and Enrique García-España*[b]

[a] Molecular Design and Synthesis, Department of Chemistry, KU Leuven, Celestijnenlaan 200f – bus 02404, 3001 Leuven, Belgium

[b] Instituto de Ciencia Molecular, Departamento de Química Inorgánica, Universidad de Valencia, C/Catedrático José Beltrán 2, 46980 Paterna, Valencia, Spain

‡ Current address: Institute of Nanoscience & Nanotechnology, NCSR ''Demokritos'', Terma Patr. Gregoriou & Neapoleos, Aghia Paraskevi, 15310, Attikis, Greece.

Contents

General experimental methods

Chemicals were purchased from Acros Organics, Sigma Aldrich, Alfa Aesar or TCI Europe and used as received. 8-(2,6-Dichlorophenyl)-BODIPY **1** was prepared according to published literature procedures, through a water based dipyrromethane synthesis followed by oxidation and condensation.[1] 5-Phenyl-8-(2,6-dichlorophenyl)-BODIPY **2** was synthesized via a reported ferrocene catalyzed radical arylation with benzenediazonium tetrafluoroborate[2] and 5-cyclohexyl-8-(2,6-dichlorophenyl)-BODIPY **3** was synthesized via a reported oxidative radical alkylation with potassium cyclohexyltrifluoroborate.[3] All reactions were carried out in flame dried glassware, but no special precautions were taken for the exclusion of moisture. Solvents were not dried prior to use.

^{1}H NMR spectra were recorded at room temperature in $CDCl_3$ on a Bruker Avance 300 instrument operating at a frequency of 300 MHz. ^{13}C NMR spectra were recorded at room temperature in $CDCl_3$ on a Bruker 400 instrument operating at a frequency of 100 MHz for ^{13}C. Due to the small coupling constants in pyrrolic dyes, the multiplicity of the signals is often unclear. In these cases, NMR signals often appear as singlets, whereas they are not. ^{1}H NMR spectra in $CDCl_3$ were referenced to tetramethylsilane (0.00 ppm) as an internal standard. ^{13}C NMR spectra in $CDCl_3$ were referenced to the $CDCl_3$ (77.16 ppm) signal.

Low resolution mass spectra were recorded on a Thermo Finnigan LCQ Advantage instrument (ESI mode). High-resolution mass data were obtained with a Waters Synapt G2 HDMS quadrupole orthogonal acceleration time-of-flight mass spectrometer (ESI mode), for which samples together with a small amount of copper(II) acetate were infused at 3 µL/min and spectra were obtained in positive ionization mode with a resolution of 15000 (fwhm) using leucine enkephalin as lock mass. Melting points were taken on a Reichert Thermovar and are uncorrected.

pH Titration experiments were carried out at room temperature in doubly distilled water that was passed through a Millipore apparatus. The pH of the solution was monitored with a Mettler Toledo SevenGo portable pH meter, and was adjusted by adding diluted HCl and NaOH solutions. All other experiments were done in 50 mM sodium cacodylate buffer (pH 5 or 7.4) made from doubly distilled water that was passed through a Millipore apparatus. All experiments were done with 10 µM solutions of the ligands in water, and these solutions were made from a 1mM stock solution in methanol. NaCl, $MnSO_4{\cdot}H_2O$, $FeCl_3{\cdot}6H_2O$, $CoCl_2{\cdot}6H_2O$, $NiCl_2{\cdot}6H_2O$, $Cu(ClO_4)_2$, $Zn(ClO_4)_2$, $CdCl_2$, $HgCl_2$ and $Pb(NO_3)_2$ were used as the sources of the corresponding metal ions.

UV−vis absorption spectra were recorded on an Agilent 8453 UV-visible spectroscopy system. The emission spectra were recorded with a PTI MO-5020 spectrofluorimeter and the raw fluorescence data were, in the case of the pH titration experiments, corrected for absorption and volume changes that occurred during the titration. The HypSpec program was used to calculate protonation and stability constants from the obtained spectroscopic data[4] and the HySS program was used to calculate the species distribution diagrams from these protonation and stability constants.[5] Absolute fluorescence quantum yields were determined with a Hamamatsu C9920–02 absolute photoluminescence quantum yield measurement system with an excitation wavelength of 472 nm using an integrating sphere accessory.

HeLa cells were grown in different 60 mm plates with DMEN medium (Gibco) supplemented with 10% FBS, 1% penicillin-streptomycin and 0.1% of fungicide, and incubated in an atmosphere of 5% CO_2 at 37 ^oC for 24 h. Then the cells were washed with PBS (Gibco) and the medium restored including the compounds in different concentrations (0, 1, 3, 5, 10, 20, 30, 40, and 50 µM) and continued incubating the cells at same conditions for 24 hours. Afterwards, the cells were washed with PBS, harvested by trypsinization (Gibco) and centrifuged at 1500 rpm for 5 min at 25 ^oC. Then $0.5*10^6$ cells/mL were re-suspended in 0.5 mL of supplemented medium and treated for analysis by flow cytometry. The same procedure was used to obtain de fluorescence images after 48 hours incubation, but in this case only three concentrations of ligands (0, 5, and 30 µM) were used.

At the cytometer (BD LSRFortessa) the fluorescent intensity was measured by excitation at 488 nm, thus the cells were distinguished between living cells with the internalised compounds (thanks to the emission of the BODIPY, λ_{em} = 550-570 nm, due to the structure of **4** and **5**, and measured with the fluorescent scatter detector FitC-A) and dead cells (stained with Propidium iodide, λ_{em} = 617 nm, which binds to apoptotic/necrotic cells with disrupted cell membranes and measured with de fluorescent scatter detector PerCP-CY5-5-A). Then the cells were gated as three types, and we could differentiate clearly living cells (blue gate) and dead cells (red gate) (A) and living cells with the compound inside (green gate) and dead cells with or without compound inside them (red gate) (B). The results were quantified using BDFACSDiva software version 7.0. The fluorescence microscope used was Nikon eclipse TE20000-S with a Mercury Lamp (λ_{ex} = 480-500 nm), which can excite both ligands, and the emission has a maximum in the green area (550 nm) and in the red area (620 nm). Therefore, the HeLa cells with compound inside can be observed.

Synthesis and characterization data

3-(2-(Bis(2-aminoethyl)amino)ethylamino)-5-phenyl-8-(2,6-dichlorophen-1-yl)-4,4-difluoro-4-bora-3a,4a-diaza-*s*-indacene 4

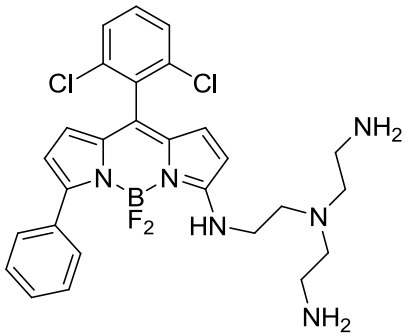

5-Phenyl-8-(2,6-dichlorophenyl)-BODIPY2 **2** (61.8 mg, 0.15 mmol) was dissolved in DMF (1.5 mL). To this solution was added tris(2-aminoethyl)amine (TREN) (90 µL, 0.6 mmol, 4 equivalents). Afterwards, the reaction mixture was stirred at room temperature under an oxygen atmosphere for 30 minutes. Subsequently, the reaction was poured in dichloromethane (100 mL), washed two times with water to a neutral pH (100 mL), dried over $MgSO_4$, filtered, and evaporated to dryness. The crude product was purified by column chromatography (silica; $CHCl_3$/NH_3 (7N in MeOH); 85:15 v/v) providing a red solid

with a green luster (48.9 mg, 59%). Mp: product is not crystalline; ^{1}H NMR ($CDCl_3$, 300 MHz): δ 7.83 (d, *J* = 7.1 Hz, 2H), 7.48–7.28 (m, 6H), 6.64 (d, *J* = 5.0 Hz, 1H), 6.38 (d, *J* = 3.8 Hz, 1H), 6.17 (t, *J* = 4.0 Hz, 2H), 3.45 (t, *J* = 5.6 Hz, 2H), 2.92 (s, br, 5H), 2.83–2.71 (m, 6H), 2.57 (t, *J* = 5.5 Hz, 4H) ppm; ^{13}C NMR ($CDCl_3$, 100 MHz): δ 161.3, 147.6, 136.5, 134.6, 133.7, 133.5, 133.3, 132.5, 130.5, 129.1, 128.2, 127.9, 127.8, 125.4, 119.1, 115.6, 111.9, 56.1, 53.7, 42.3, 39.6 ppm; MS (ESI, *m/z*): 557 (M + H^+); HRMS (ESI-TOF) m/z: $[M + H]^+$ calcd for $C_{27}H_{30}BCl_2F_2N_6$ 557.1970, found 557.1976; $[M - F]^+$ calcd for $C_{27}H_{29}BCl_2FN_6$ 537.1908, found 537.1917.

3-(2-(Bis(2-aminoethyl)amino)ethylamino)-5-cyclohexyl-8-(2,6-dichlorophen-1-yl)-4,4-difluoro-4-bora-3a,4a-diaza-*s*-indacene 5

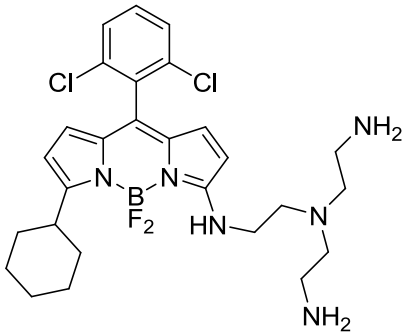

5-Cyclohexyl-8-(2,6-dichlorophenyl)-BODIPY3 **3** (62.7 mg, 0.15 mmol) was dissolved in DMF (1.5 mL). To this solution was added tris(2-aminoethyl)amine (TREN) (90 µL, 0.6 mmol, 4 equivalents). Afterwards, the reaction mixture was stirred at room temperature under an oxygen atmosphere for 3 hours. Subsequently, the reaction was poured in dichloromethane (100 mL), washed two times with water to a neutral pH (100 mL), dried over $MgSO_4$, filtered, and evaporated to dryness. The crude product was purified by column chromatography (silica; $CHCl_3$/NH_3 (7N in MeOH); 85:15 v/v) providing an orange solid with a green luster (55.2 mg, 65%). Mp: product is not crystalline; ^{1}H NMR ($CDCl_3$, 300 MHz): δ 7.45–7.28 (m, 3H), 6.58 (d, *J* = 4.9 Hz, 1H), 6.23–5.93 (m, 3H), 3.47 (t, *J* = 5.7 Hz, 2H), 3.11–2.99 (m, 1H), 2.87 (t, *J* = 5.6 Hz, 4H), 2.79 (t, *J* = 5.7 Hz, 2H), 2.63 (t, *J* = 5.6 Hz, 4H), 2.11 (d, *J* = 10.9 Hz, 2H), 1.88–1.70 (m, 3H), 1.47–1.26 (m, 5H) ppm; ^{13}C NMR ($CDCl_3$, 100 MHz): δ 160.7, 156.9, 136.4, 133.0, 132.7, 132.5, 130.6, 130.3, 128.1, 126.2, 119.9, 110.9, 110.0, 56.7, 53.7, 42.1, 39.8, 38.0, 33.9, 26.9, 26.4 ppm; MS (ESI, *m/z*): 563 (M + H^+); HRMS (ESI-TOF) m/z: $[M + H]^+$ calcd for $C_{27}H_{36}BCl_2F_2N_6$ 563.2440, found 563.2452; $[M - F]^+$ calcd for $C_{27}H_{35}BCl_2FN_6$ 543.2377, found 543.2379.

NMR spectra of new compounds

4, ^{1}H, 300 MHz, $CDCl_3$

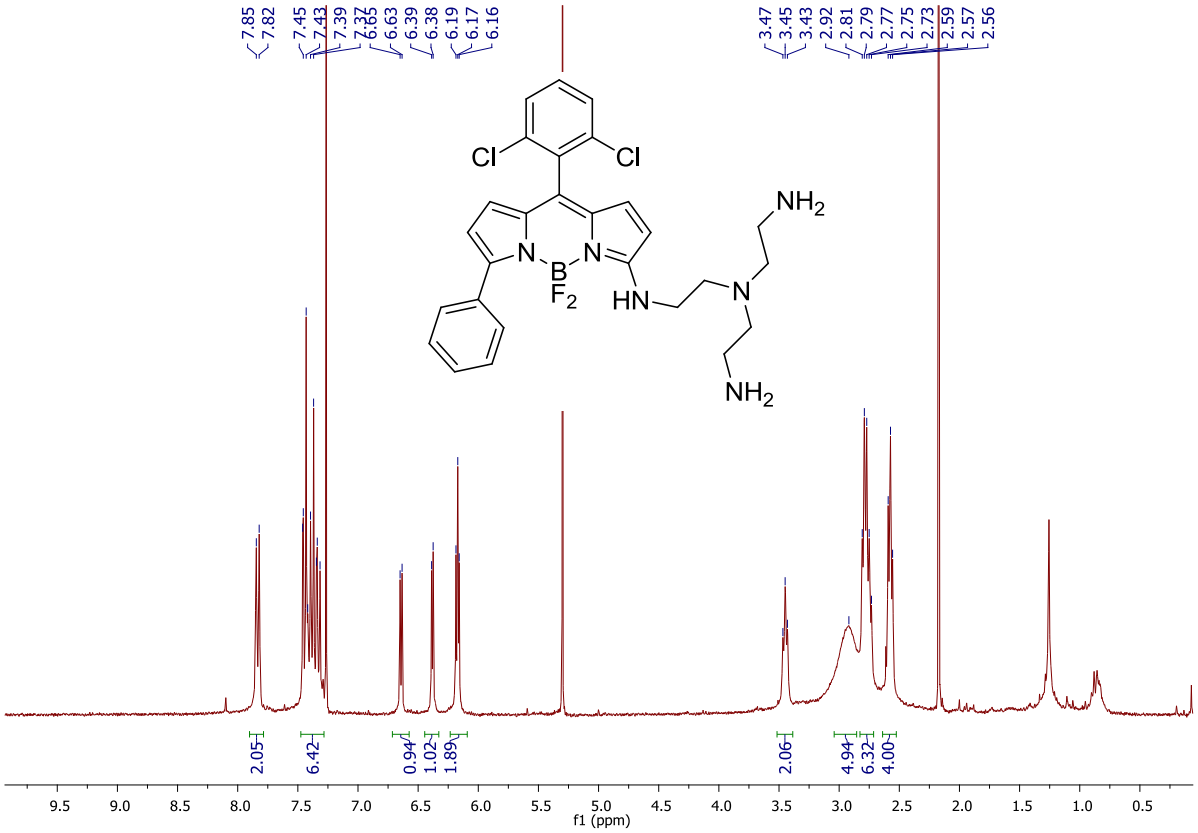

4, ^{13}C, 100 MHz, $CDCl_3$

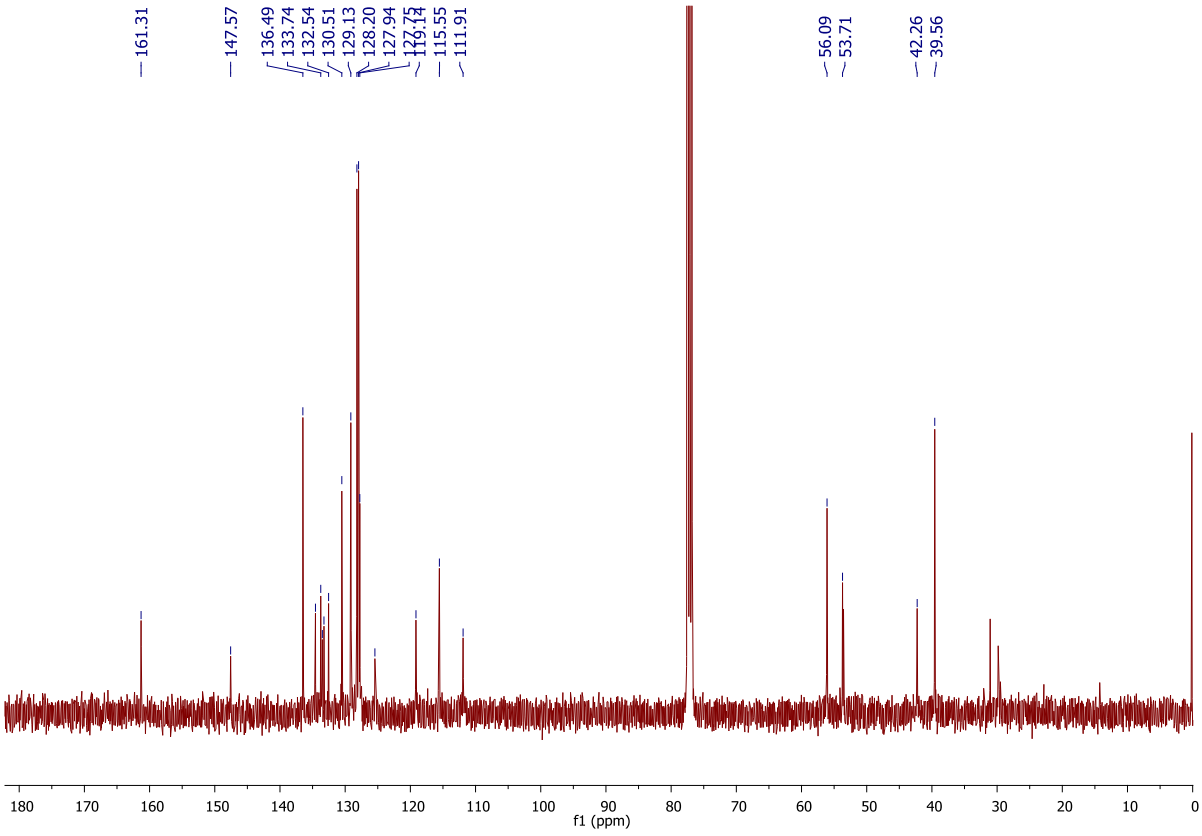

5, ^{1}H, 300 MHz, $CDCl_3$

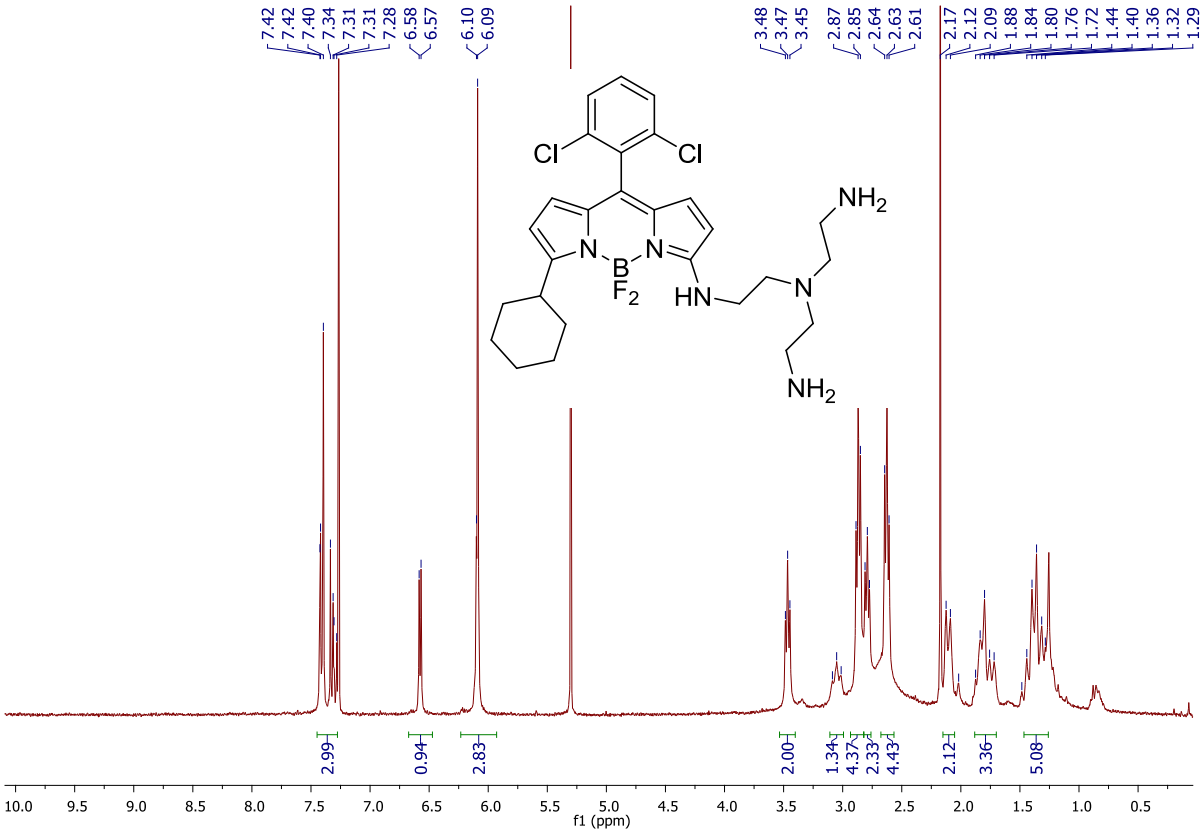

5, ^{13}C, 100 MHz, $CDCl_3$

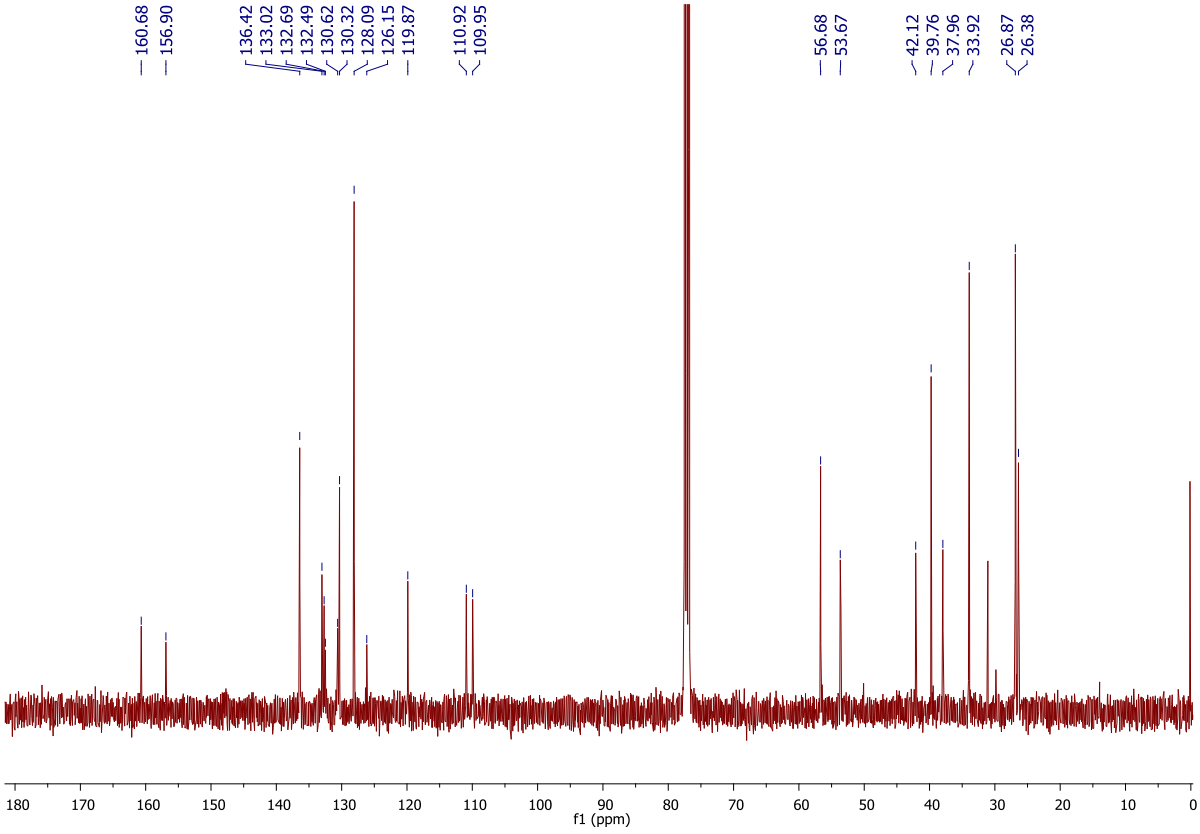

Spectroscopic data

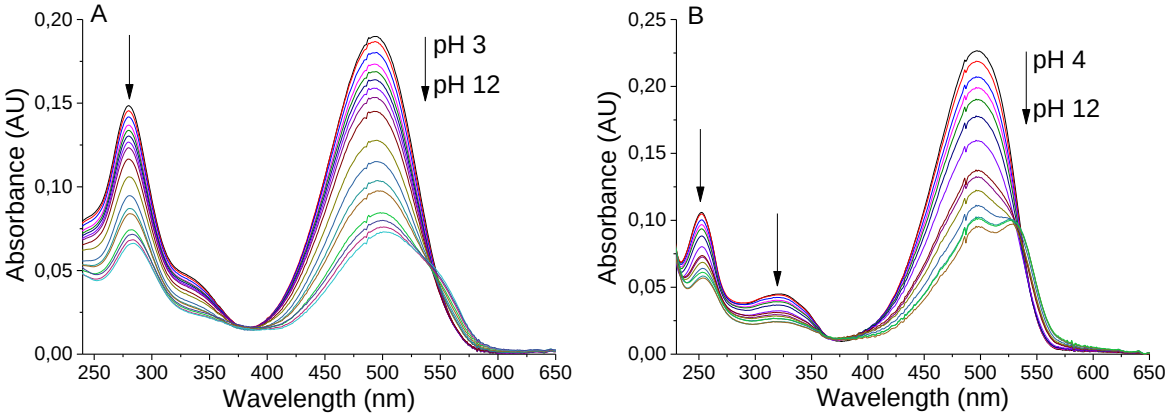

Figure S1: pH-Dependence of the UV–vis absorption spectra of compounds (A) **4** (10 µM) and (B) **5** (10 µM) in water.

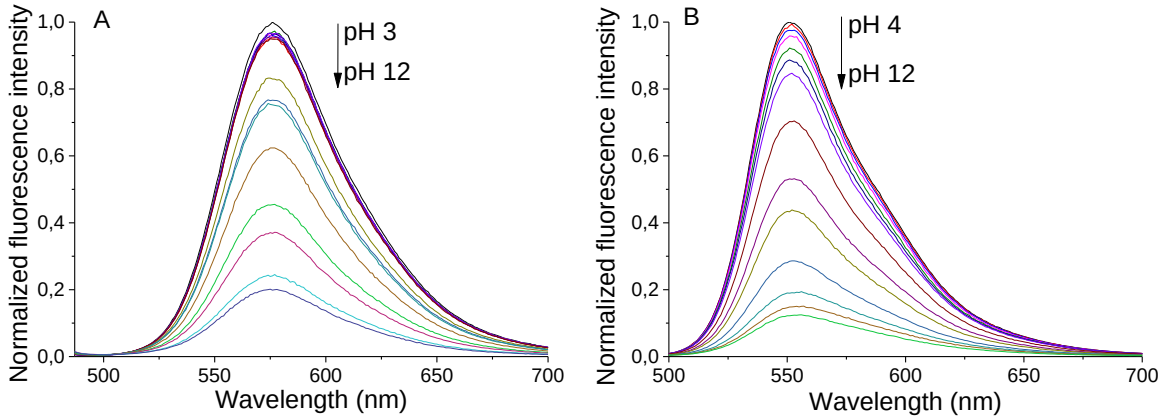

Figure S2: pH-Dependence of the fluorescent emission spectra of compounds (A) **4** (10 µM, λ_{ex} = 472 nm) and (B) **5** (10 µM, λ_{ex} = 472 nm) in water.

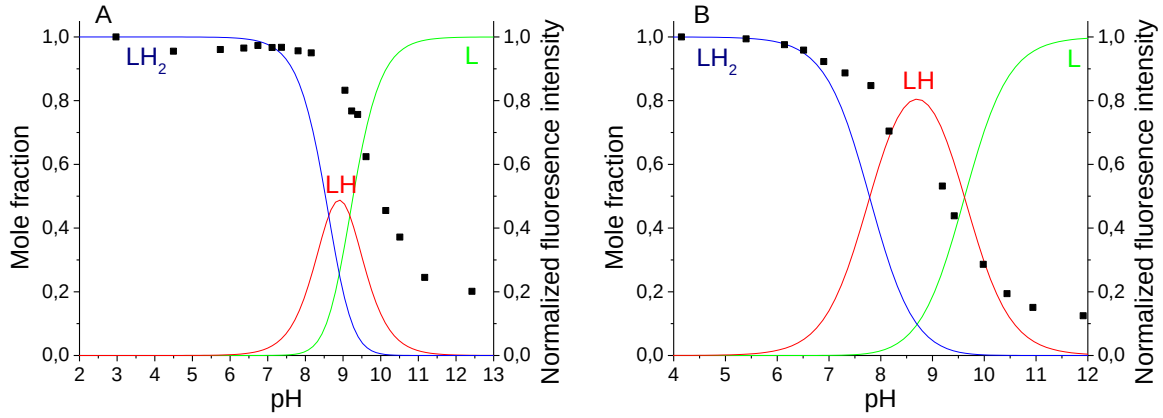

Figure S3: Fluorescence emission pH titration curve of compounds (A) **4** (10 µM, λ_{ex} = 472 nm, λ_{em} = 576 nm) and (B) **5** (10 µM, λ_{ex} = 472 nm, λ_{em} = 552 nm) in water (black ■) and mole fraction distribution diagrams for the various protonated species of these ligands (solid lines).

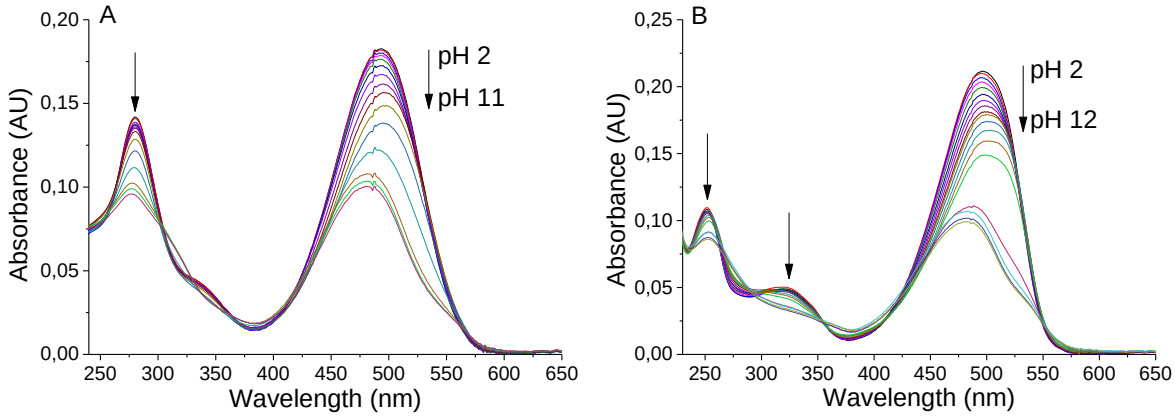

Figure S4: pH-Dependence of the UV–vis absorption spectra of compounds (A) **4** (10 µM) and (B) **5** (10 µM) in water in the presence of 1 equivalent of Cu(II).

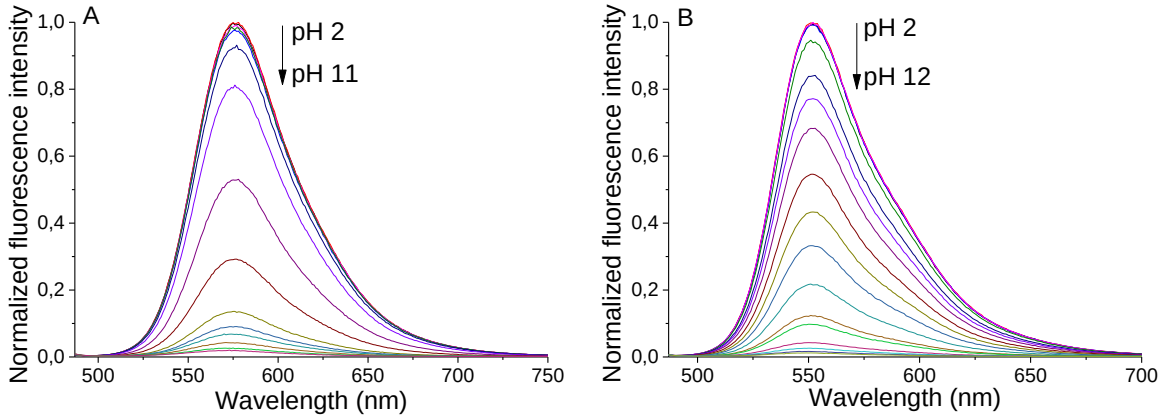

Figure S5: pH-Dependence of the fluorescent emission spectra of compounds (A) **4** (10 µM, λ_{ex} = 472 nm) and (B) **5** (10 µM, λ_{ex} = 472 nm) in water in the presence of 1 equivalent of Cu(II).

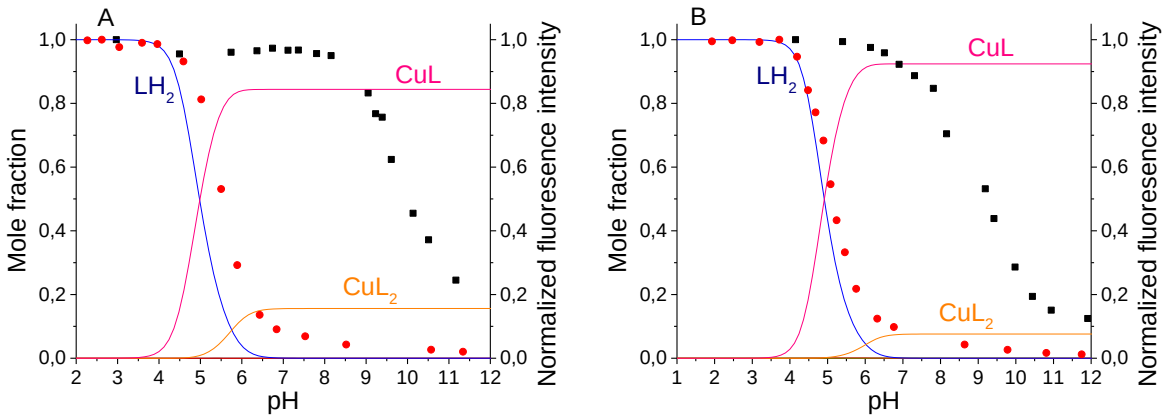

Figure S6: Fluorescence emission pH titration curve of compounds (A) **4** (10 µM, λ_{ex} = 472 nm, λ_{em} = 576 nm) and (B) **5** (10 µM, λ_{ex} = 472 nm, λ_{em} = 552 nm) in water in the absence (black ■) or presence of 1 equivalent of Cu(II) (red ●) and mole fraction distribution diagrams for the various species of these ligands in presence of 1 equivalent of Cu(II) (solid lines).

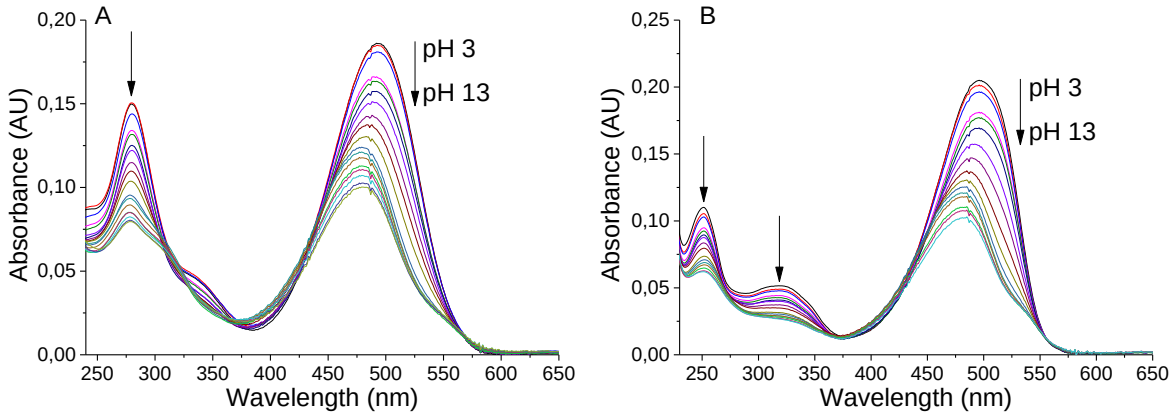

Figure S7: pH-Dependence of the UV–vis absorption spectra of compounds (A) **4** (10 µM) and (B) **5** (10 µM) in water in the presence of 1 equivalent of Zn(II).

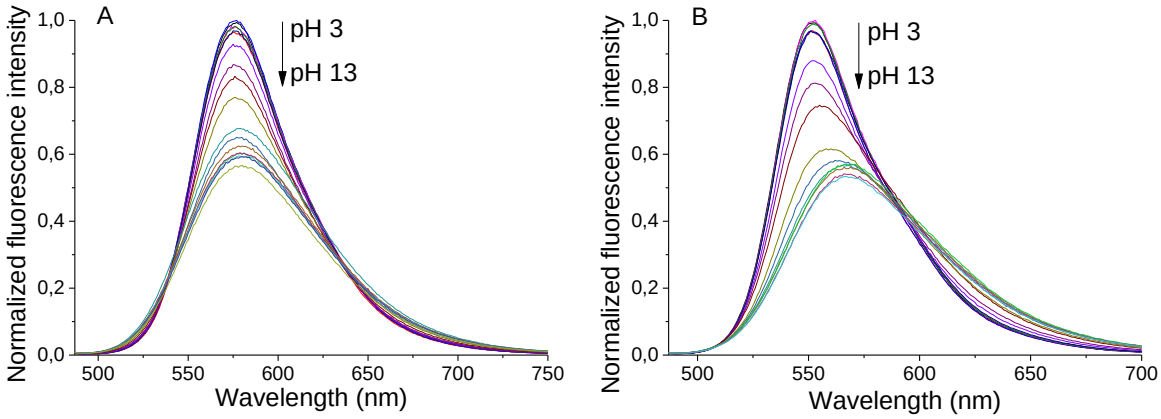

Figure S8: pH-Dependence of the fluorescent emission spectra of compounds (A) **4** (10 µM, λ_{ex} = 472 nm) and (B) **5** (10 µM, λ_{ex} = 472 nm) in water in the presence of 1 equivalent of Zn(II).

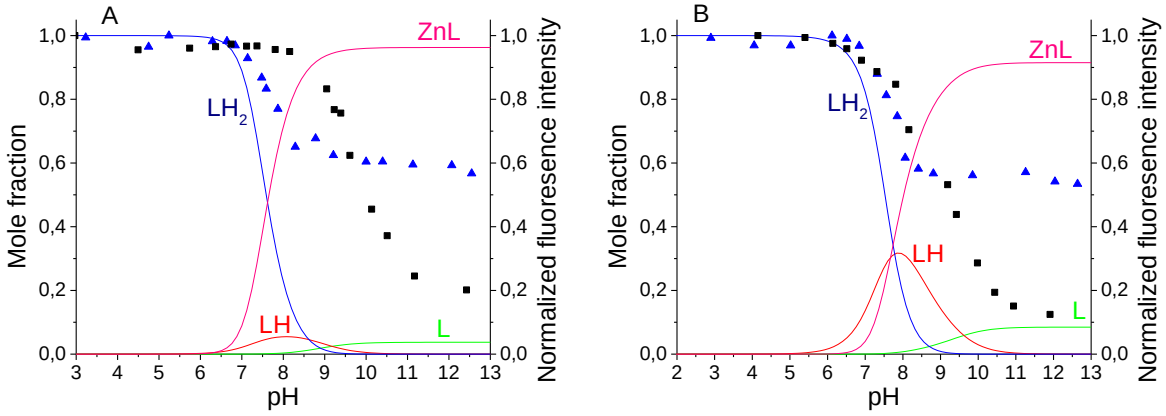

Figure S9: Fluorescence emission pH titration curve of compounds (A) **4** (10 µM, λ_{ex} = 472 nm, λ_{em} = 576 nm) and (B) **5** (10 µM, λ_{ex} = 472 nm, λ_{em} = 552 nm) in water in the absence (black ■) or presence of 1 equivalent of Zn(II) (blue ▲) and mole fraction distribution diagrams for the various species of these ligands in presence of 1 equivalent of Zn(II) (solid lines). Charges omitted.

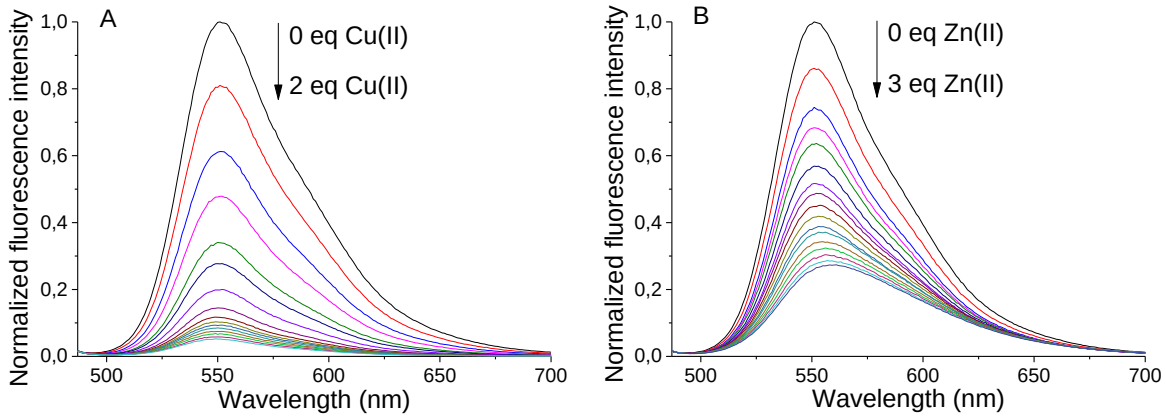

Figure S10: Influence of (A) Cu(II) and (B) Zn(II) concentration on the fluorescent emission spectra of compound **5** (10 µM, λ_{ex} = 472 nm) in an aqueous sodium cacodylate buffer solution (0.05 M, pH 7.4).

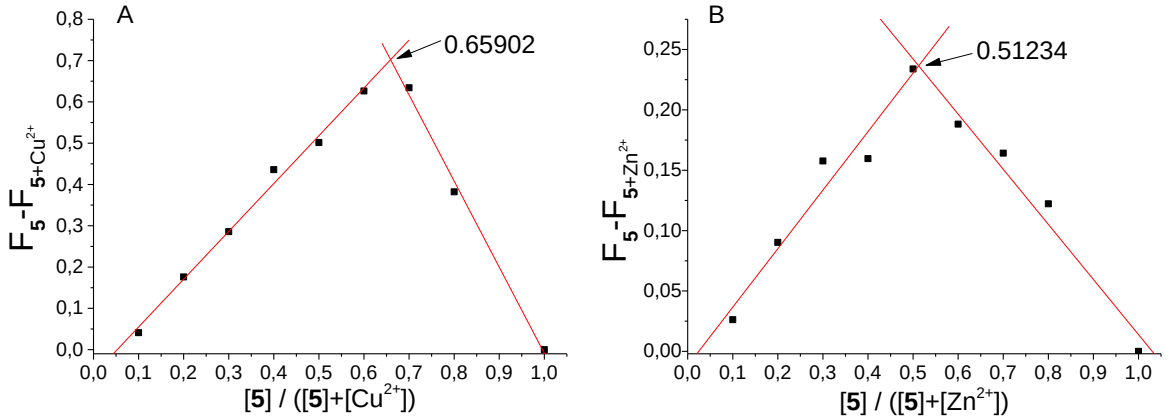

Figure S11: Job plot of ligand **5** (λ_{ex} = 472 nm, λ_{em} = 552 nm) with (A) Cu(II) and (B) Zn(II) in an aqueous sodium cacodylate buffer solution (0.05 M, pH 7.4). The total concentration of ligand and metal ion was 10 µM. $F_{\mathbf{5}}$, $F_{\mathbf{5}+Cu^{2+}}$ and $F_{\mathbf{5}+Zn^{2+}}$ denote the normalized fluorescence intensity of the free ligand, the ligand in the presence of Cu(II) and in the presence of Zn(II), respectively.

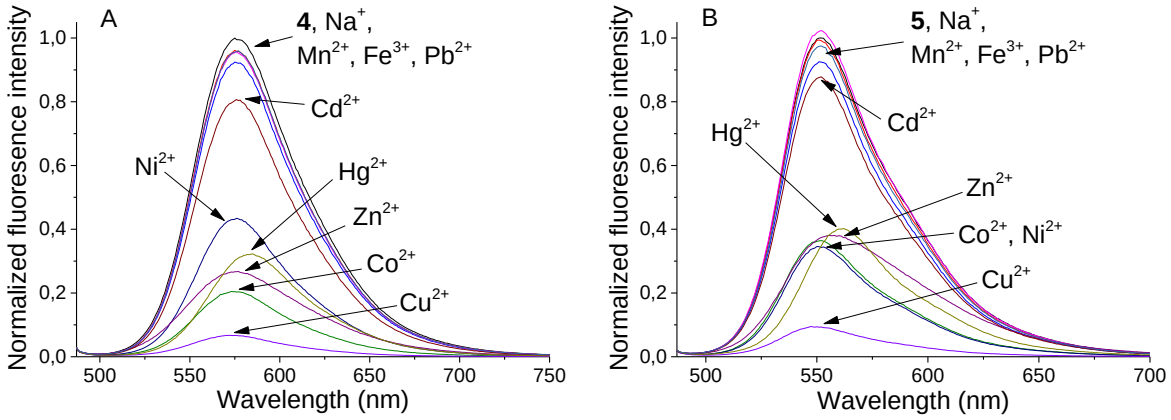

Figure S12: Influence of a selection of metal ions on the fluorescent emission spectra of compounds (A) **4** (10 µM, λ_{ex} = 472 nm) and (B) **5** (10 µM, λ_{ex} = 472 nm) in an aqueous sodium cacodylate buffer solution (0.05 M, pH 7.4)

Flow cytometry data

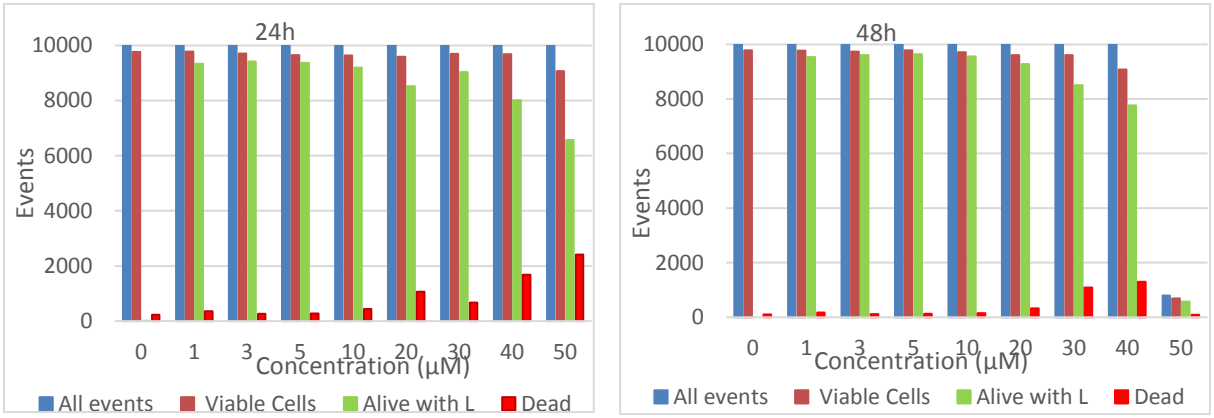

Figure S13: HeLa cells viability incubated with ligand **4** for 24 hours at 37°C (left), and for 48 hours (right).

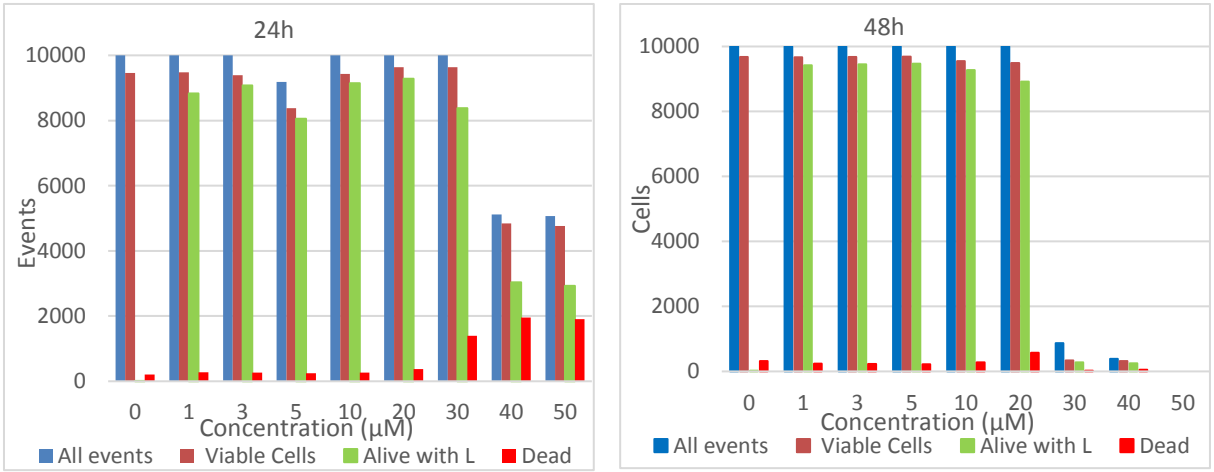

Figure S14: HeLa cells viability incubated with ligand **5** for 24 hours at 37°C (left), and for 48 hours (right).

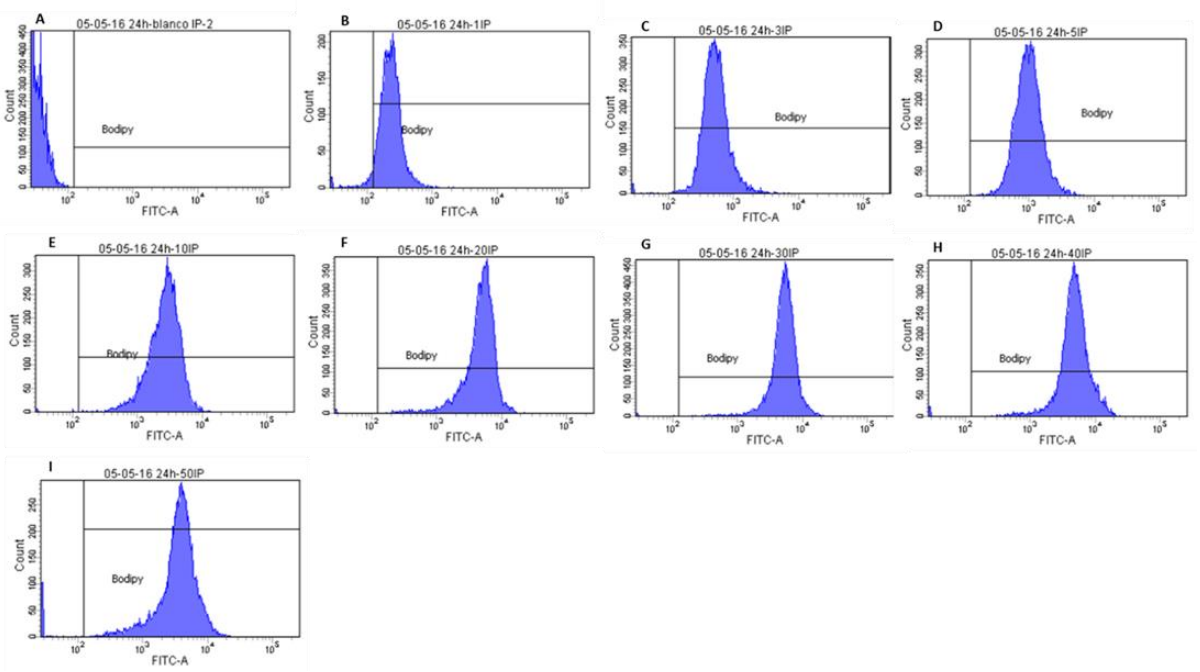

Figure S15: Emission of the compound **4** at 24 hours for different concentrations: A) Control, B) 1 µM of compound, C) 3 µM, D) 5 µM, E) 10 µM, F) 20 µM, G) 30 µM, H) 40 µM, I) 50 µM. This data was obtained from the individual emission of each sample acquired by the fluorescence detector (FITC-A) of the cytometer, showing that the amount of emission of the living cells increases as long as de concentration of the compound inside de cell increases too, until 40 µM.

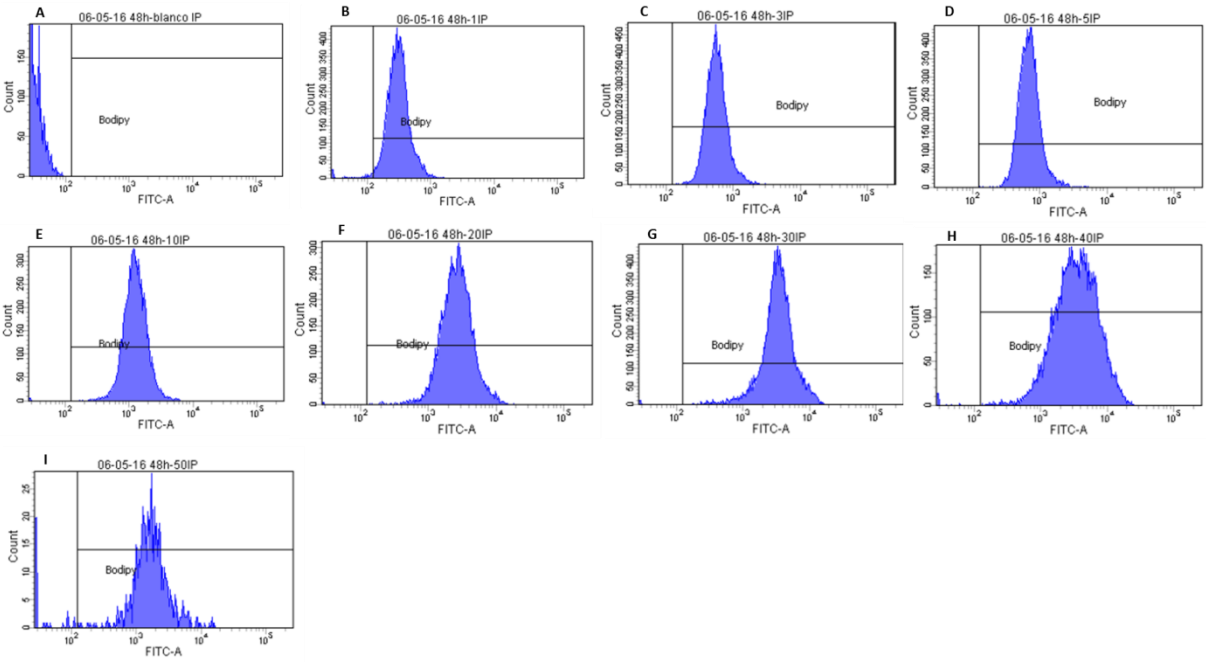

Figure S16: Emission of the compound **4** at 48 hours for different concentrations: A) Control, B) 1 µM of compound, C) 3 µM, D) 5 µM, E) 10 µM, F) 20 µM, G) 30 µM, H) 40 µM, I) 50 µM. This data was obtained from the individual emission of each sample acquired by the fluorescence detector (FITC-A) of the cytometer, showing that the amount of emission of the living cells increases as long as de concentration of the compound inside de cell increases too, until 40 µM. At 50 µM there were not almost living cells.

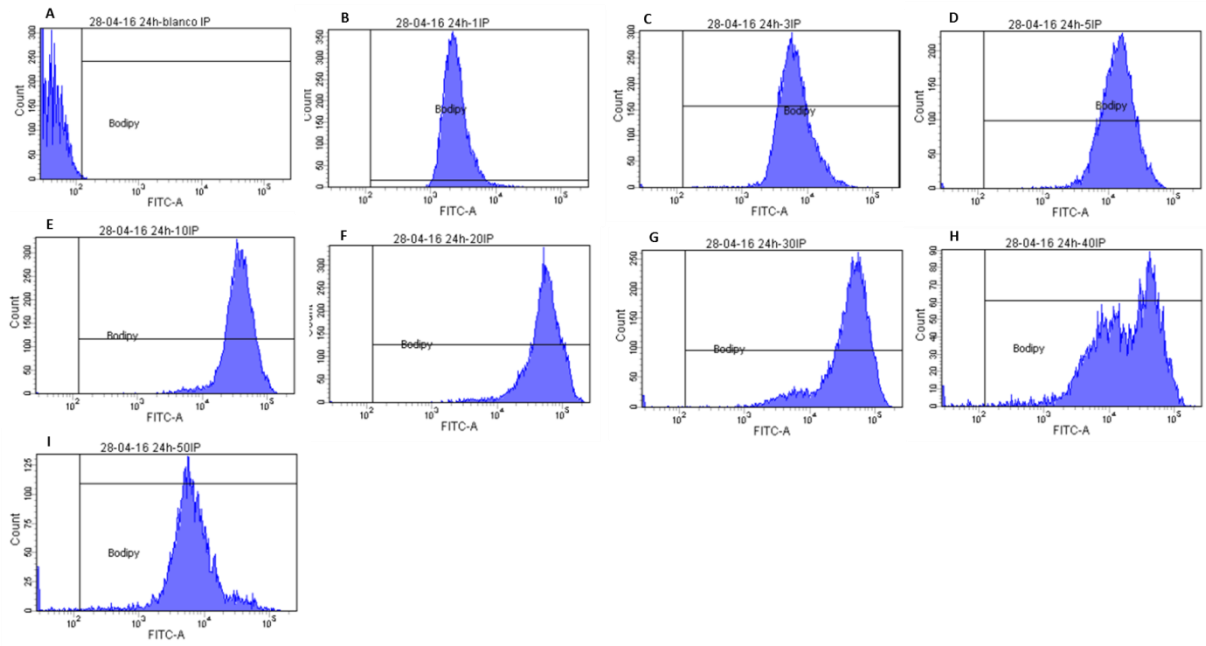

Figure S17: Emission of the compound **5** at 24 hours for different concentrations: A) Control, B) 1 µM of compound, C) 3 µM, D) 5 µM, E) 10 µM, F) 20 µM, G) 30 µM, H) 40 µM, I) 50 µM. This data was obtained from the individual emission of each sample acquired by the fluorescence detector (FITC-A) of the cytometer, showing that the amount of emission of the living cells increases as long as de concentration of the compound inside de cell increases too, until 30 µM. Then for 40 µM and 50 µM there were not enough living cells (Figure S14).

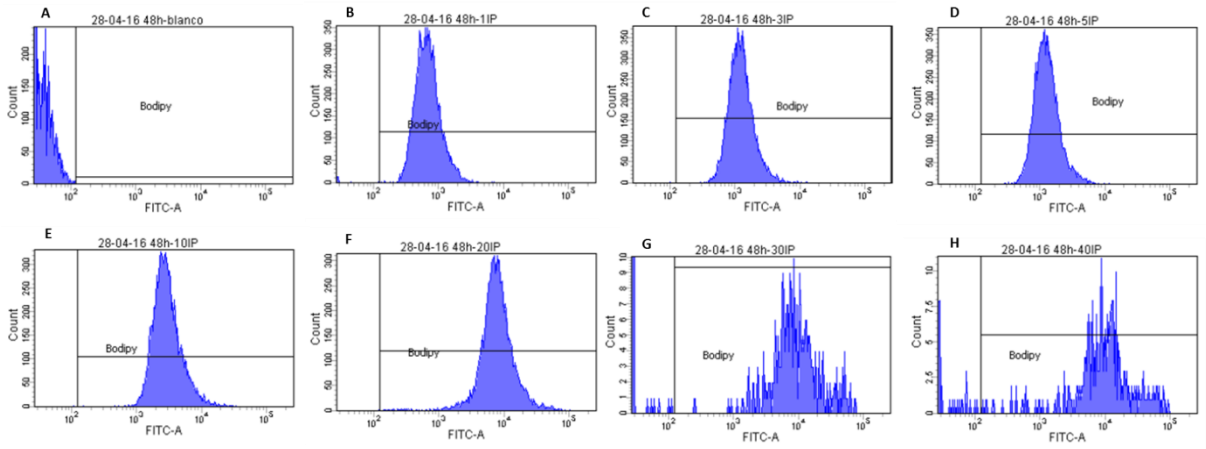

Figure S18: Emission of the compound **5** at 48 hours for different concentrations: A) Control, B) 1 µM of compound, C) 3 µM, D) 5 µM, E) 10 µM, F) 20 µM, G) 30 µM, H) 40 µM, I) 50 µM. This data was obtained from the individual emission of each sample acquired by the fluorescence detector (FITC-A) of the cytometer, showing that the amount of emission of the living cells increases as long as de concentration of the compound inside de cell increases too, until 20 µM. Then for 30 µM and 40 µM there were not enough living cells, and there was no cell at 50 µM. (Figure S14).

Confocal fluorescence images

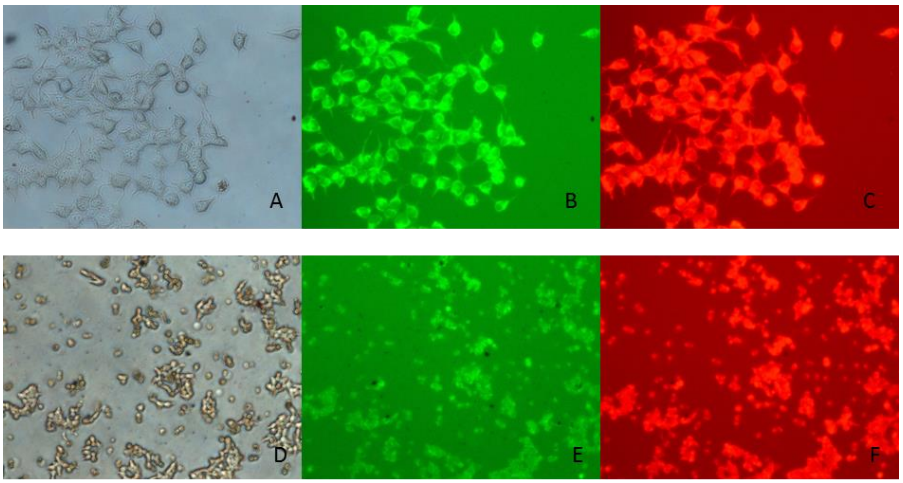

Figure S19: Fluorescence images of HeLa cells grown with ligand **4** at 5 µM (A, B and C) and 30 µM (D, E and F), incubated for 24 hours. At 30 µM cells many were damaged and their structure changed.

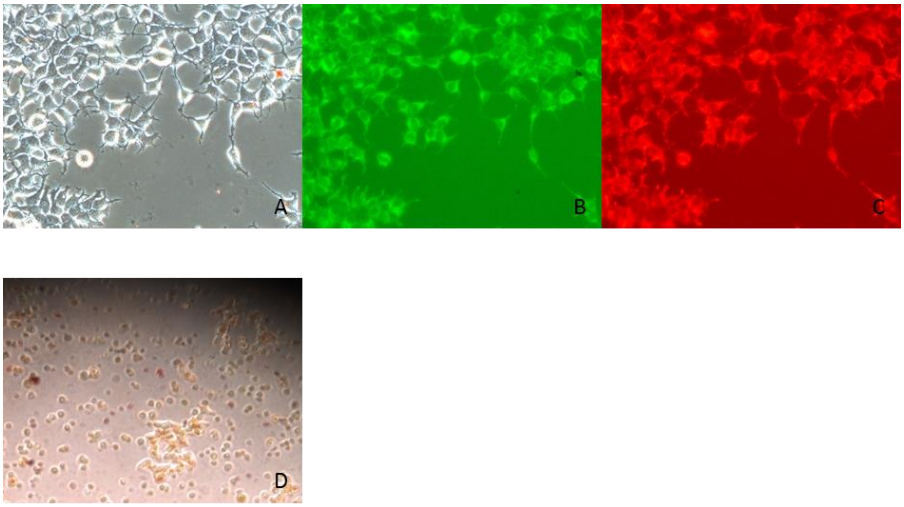

Figure S20: Fluorescence images of HeLa cells grown with ligand **4** at 5 µM (A, B and C) and 30 µM (D), incubated for 48 hours.

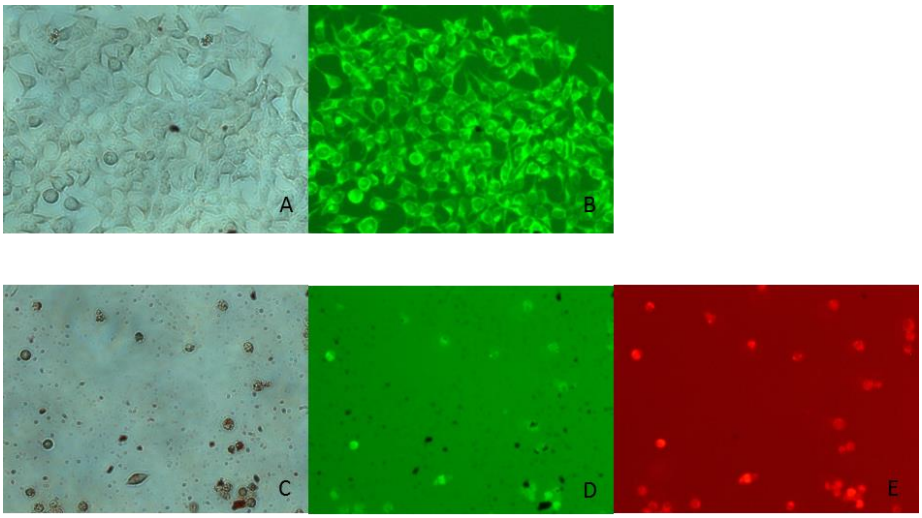

Figure S21: Fluorescence images of HeLa cells grown with ligand **5** at 5 µM (A, B) and 30 µM (C, D and E), incubated for 24 hours. At 30 µM the number of cells was less.

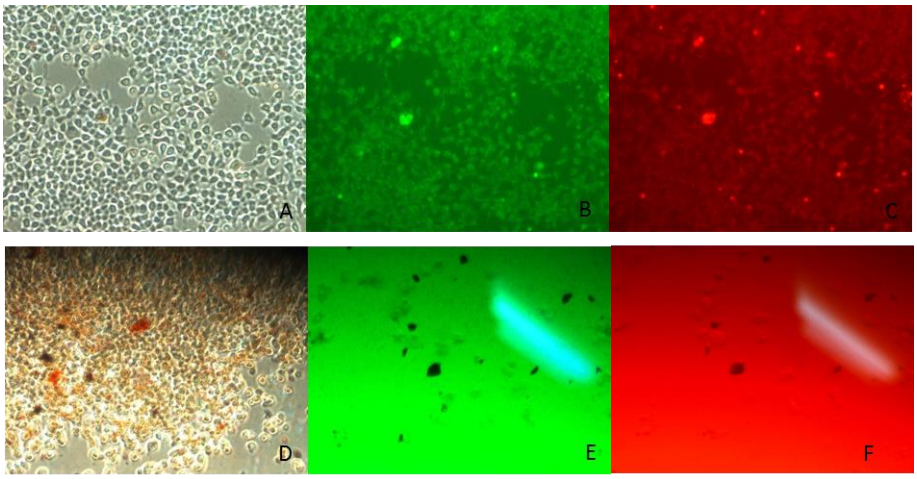

Figure S22: Fluorescence images of HeLa cells grown with ligand **5** at 5 µM (A, B and C) and 30 µM (D, E and F), incubated for 48 hours. At 30 µM the cells were damaged and there was no emission.

References

1 V. Leen, M. Van der Auweraer, N. Boens and W. Dehaen, *Org. Lett.*, 2011, **13**, 1470–1473.
2 B. Verbelen, S. Boodts, J. Hofkens, N. Boens and W. Dehaen, *Angew. Chem. Int. Ed.*, 2015, **54**, 4612– 4616.
3 B. Verbelen, L. C. D. Rezende, S. Boodts, J. Jacobs, L. Van Meervelt, J. Hofkens and W. Dehaen, *Chem. Eur. J.*, 2015, **21**, 12667–12675.
4 (a) P. Gans, A. Sabatini and A. Vacca, *Talanta*, 1996, **43**, 1739–1753 ; (b) P. Gans, A. Sabatini and A. Vacca, *Ann. Chim.*, 1999, **89**, 45–49.
5 L. Alderighi, P. Gans, A. Ienco, D. Peters, A. Sabatini and A. Vacca, *Coord. Chem. Rev.*, 1999, **184**, 311–318.